Determination of Orientational Order Parameters of Two Tri-Component Mixtures from Optical Birefringence and X-Ray Diffraction Measurements

S. Basak[a], P. Dasgupta[a], B. Das[a,*], M.K. Das[b] and R. Dabrowski[c]

[a]Department of Physics, Siliguri Institute of Technology, Siliguri, Darjeeling — 734 009, India

[b]Department of Physics, University of North Bengal, Siliguri, Darjeeling — 734 013, India

[c]Department of Advanced Technologies and Chemistry, Military University of Technology, 00-908 Warsaw, Poland

Two tri-component mixtures as base mixtures for vertically aligned mode LCD's were prepared. The eutectic compositions were theoretically estimated and experimentally verified from differential scanning calorimetry studies. A room temperature nematic mixture with fairly broad operating range emerged from each of the tri-component mixtures. The optical birefringence of these mixtures at the eutectic composition was measured as a function of temperature. X-ray diffraction measurements were done on these mixtures to obtain the orientational order parameters as a function of temperature. The order parameter values were also determined from birefringence measurements and the results were compared with mean field theory. Structural parameters like intermolecular distance and apparent molecular length have also been determined.

PACS: 61.05.cp, 61.30.−v, 42.70.Df

1. Introduction

The conventional twisted nematic liquid crystal displays (TN-LCD's) use liquid crystal materials with positive dielectric anisotropy. However, the greatest drawbacks of the TN LCD's are their narrow viewing angle, low contrast and slow response times. In contrast, the vertically aligned (VA) mode LCD's [1–5], based on liquid crystal materials with negative dielectric anisotropy, offers a superior picture quality with wide viewing angle [6, 7], high contrast [8] and video-compatible switching times [9, 10]. Liquid crystalline materials suitable for VA mode LCD's are mainly focused on dielectrically negative fluorinated liquid crystals comprising of 1,2-difluorobenzene building block [11] which combine the necessary polarity with chemical stability and low polarizability [12, 13] suitable for their application in VA mode LCD's. Difluorinated alkoxy compounds are suitable for preparation of VA mixtures because of their large negative dielectric anisotropy and low optical birefringence. Moreover, the recently synthesized terphenyl derivatives with lateral fluorine substitution have the additional advantage of low rotational viscosity, while keeping the birefringence moderately low as required for VA mode applications [14].

In this work, four compounds constituting the main components of the mixture for vertical alignment were

chosen. The phase diagram of one bi-component mixture comprising of two terphenyl derivatives and two tri-component systems comprising of terphenyl derivatives and bicyclohexane compounds were studied. The molar composition of the individual components of the tri-component system was theoretically estimated and both the theoretical and experimental eutectic points for the tri-component mixtures were compared.

The order parameter in nematic liquid crystals is one among the most important physical parameters [15–17] which dictate its performance in display devices. The material properties of liquid crystals, viz. the dielectric, optical and magnetic anisotropies depend on the order parameter in a more or less straightforward way. Thus, it is of great importance to study the temperature dependence of the orientational order parameters of liquid crystalline materials. Although a large volume of work has been reported in the literature on the determination of orientational order parameters of pure compounds as well as mixtures having positive dielectric anisotropy, such measurements on liquid crystalline systems possessing negative dielectric anisotropy, especially mixtures suitable for VA mode application, seems to be scanty.

Therefore detailed X-ray diffraction measurements were done at the eutectic compositions for both the tri-component systems. The orientational order parameter (OOP), apparent molecular length, layer spacing and intermolecular distance were determined as a function of temperature. The optical birefringence (Δn) was determined as a function of temperature. The temperature de-

---

* corresponding author; e-mail: `banbuin@yahoo.com`

pendence of the birefringence was also used to determine the orientational order parameter. The orientational order parameters determined from X-ray and birefringence measurement have been compared with the Maier–Saupe mean field theory [18].
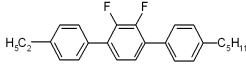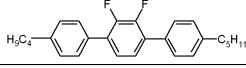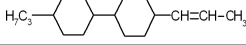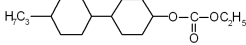
2. Experimental

2.1. Materials

The chemical structure, transition temperatures and transition enthalpies (as obtained from DSC measurements) of the main components of VA mixtures are shown in Table I.

The phase diagram of the binary system comprising of compounds A and B (A+B system) was constructed and the eutectic point was determined. The physical properties of this A+B mixture was then modified by the introduction of (i) compound C resulting in the formulation of the ABC mixture and (ii) compound D resulting in the formulation of the ABD mixture. The molar ratios of the individual compounds in the mixtures for the eutectic composition were theoretically estimated by solving the Schröder–van Laar equation [19, 20]. Differential scanning calorimetry (DSC) measurements were done on these ABC and ABD mixtures to confirm the formation of eutectic mixture and to obtain the transition temperatures and transition enthalpies.

TABLE I

Chemical structure, transition temperatures and the transition enthalpies of the pure components of the vertical alignment mixtures.

Compound No.	Structure	T_m [°C]	ΔH_m [kJ/mol]	T_C (T_{NI}) [°C]	ΔH_C [kJ/mol]
A		41.64	18.17	109.66	0.670
B		50.84	20.76	111.5	0.544
C		43.3	19.51	86.4	0.586
D		60.8	30.43	72.8	0.711

2.2. Texture and DSC studies

The phase transition temperatures and enthalpies were determined by DSC, using the SETARAM 141 calorimeter. The transition temperatures and textures were observed using polarizing optical microscope BIPOLAR PI equipped with LINKAM 660 hot stage, controlled by the TMS 93 unit. In all cases, typical thread-like textures, characteristic of the nematic phase were observed under the polarizing microscope.

2.3. Optical birefringence measurements

The optical birefringence measurements were done by measuring the intensity of a He–Ne laser beam transmitted through a homogeneously aligned cell of thickness 8.9 μm filled with liquid crystal sample and probed its phase retardation. The experimental method for the birefringence measurement from optical transmission method has been described in our earlier paper [21].

We have estimated the orientational order parameter in the liquid crystalline phases using the birefringence data. The order parameter is defined as $\langle P_2 \rangle = \Delta n / \Delta n_0$, where Δn_0 is the birefringence in the completely ordered state [22] and is determined from the temperature dependence of Δn, which can be approximated well for nematic liquid crystals by

$$\Delta n = \Delta n_0 \left(1 - \frac{T}{T_1}\right)^{\beta}, \qquad (1)$$

where Δn_0, T_1 and β are adjustable parameters. T_1 is about 1–3 K higher than the clearing temperature and exponent β depends on molecular structure and its value is close to 0.2. This method enables us to extrapolate $\Delta \alpha$ to absolute zero temperature, $\Delta \alpha_0$. The value of the fitted parameters are $\Delta n_0 = 0.2437$, $T_1 = 376.9$ K and $\beta = 0.154$ for mixture ABC and $\Delta n_0 = 0.2541$, $T_1 = 379.0$ K and $\beta = 0.162$ for mixture ABD. These values of β are typical for nematic liquid crystals.

2.4. X-ray diffraction measurements

X-ray diffraction patterns were recorded on an X-ray film using a flat plate camera at several temperatures within the mesomorphic phase using Ni-filtered Cu K_α radiation of wavelength $\lambda = 1.542$ Å. Monodomain samples were easily obtained by orienting of the nematic samples in a magnetic field of 0.4 T. The X-ray diffraction photographs were scanned by a HP Scanjet 5590. Optical densities of the pixels were calculated and then converted to X-ray intensities with the help of a calibration curve following the procedure of Klug and Alexander [23]. The

experimental setup and the procedure for order parameter determination from X-ray diffraction studies have been described earlier [24].

3. Results and discussion

The phase diagram of the A+B system is shown in Fig. 1. Also shown in Fig. 1 are the theoretically calculated temperatures using the Schröder–van Laar equation [19, 20]:

$$\ln x_k = -\frac{\Delta H_{\mathrm{m}}^k}{R}\left(\frac{1}{T} - \frac{1}{T_{\mathrm{m}}^k}\right) \tag{2}$$

under the condition

$$\sum_{k=1}^{n} x_k = 1\,, \tag{3}$$

where x_k is the molar ratio of k-component; ΔH_{m}^k and T_{m}^k are the melting enthalpy (J mol^{-1}) and the temperature values (K), respectively, and R is the universal gas constant (8.31 J mol^{-1} K^{-1}).
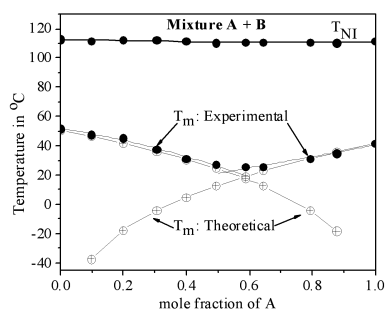

Fig. 1. Phase diagram of binary mixture A+B. From the experiment, $x_{\mathrm{eutectic}} = 0.565$, $T_{\mathrm{m}} = 22.5\,^{\circ}$C, $T_{\mathrm{c}} = 110.9\,^{\circ}$C and from the theory $x_{\mathrm{eutectic}} = 0.575$, $T_{\mathrm{m}} = 20.11\,^{\circ}$C, $T_{\mathrm{c}} = 110.9\,^{\circ}$C, where T_{m} and T_{c} are the melting and the clearing temperatures, respectively.
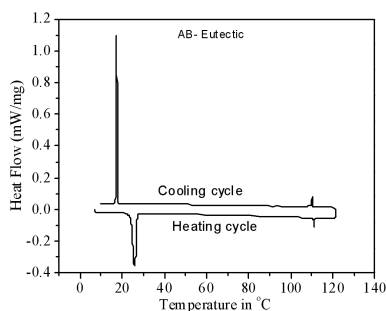

Fig. 2. DSC scans of A+B mixture at 0.565 concentration of compound A.

The theoretically estimated eutectic point is at a concentration of 0.575 mole fraction of compound A with a clearing point at 110.9 °C. The experimentally determined eutectic point was at 0.565 mole fraction of compound A with a clearing point at 110.9 °C. It is observed
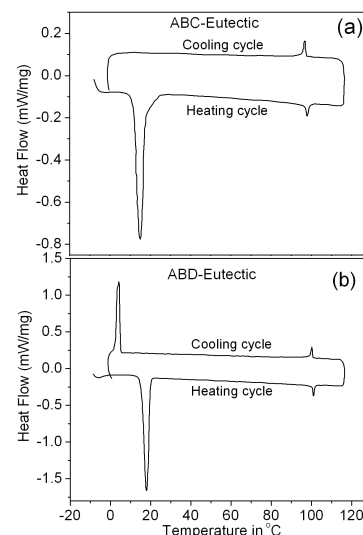

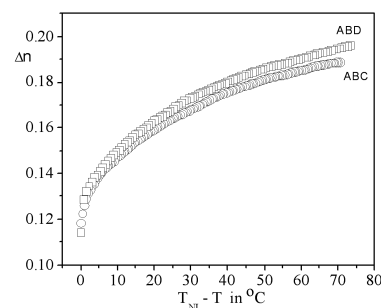Fig. 3. DSC scans of two eutectic mixtures (a) ABC, (b) ABD during heating and cooling.

Fig. 4. Birefringence values as a function of temperature $T_{\mathrm{NI}} - T$ obtained from transmission method. T_{NI} = nematic-isotropic transition temperature.

from Fig. 1 that the experimental eutectic point is concordant with the theoretically calculated values. DSC studies on the A+B mixture at 0.565 concentration of compound A confirm the formation of eutectic mixture (Fig. 2).

The eutectic composition for the tri-component mixtures A+B+C and A+B+D was also estimated using theoretical calculations from the Schröder–van Laar equation. The mixtures were prepared and DSC studies were performed to test the formation of eutectic mixtures and also whether the calculated eutectic values are in agreement with the experimental eutectic points. DSC studies confirm the formation of the eutectic mixtures (Fig. 3a,b).

The results of the DSC measurements as well as the theoretically calculated values are listed in Table II.

The experimental eutectic compositions of the bi- and tri-component systems were found to be within reasonable agreement with the theoretically calculated eutectic points. Moreover, the formation of these eutectic mix-

tures was not accompanied by the formation of inter-molecular complexes.

Results of our birefringence measurements are plotted in Fig. 4. It is seen that the birefringence values for mixture ABD at lower temperature are higher compared to ABC mixture. The values are around 0.2 which are slightly higher than those required for VA materials. The Δn values for the both mixtures near the transition temperature are nearly the same.

TABLE II

Comparison of the theoretical and experimental eutectic points.

Mixtures	Theoretical	Experimental
A+B+C	$T_{\mathrm{m}} = 3.65\,^{\circ}\mathrm{C}$ $T_{\mathrm{C}} = 102.11\,^{\circ}\mathrm{C}$	$T_{\mathrm{m}} = 11.66\,^{\circ}\mathrm{C}$, $\Delta H_{\mathrm{m}} = 20.62\,\mathrm{kJ/mol}$ $T_{\mathrm{C}} = 97.45\,^{\circ}\mathrm{C}$, $\Delta H_{\mathrm{c}} = 0.58\,\mathrm{kJ/mol}$
A+B+D	$T_{\mathrm{m}} = 12.35\,^{\circ}\mathrm{C}$ $T_{\mathrm{C}} = 104.6\,^{\circ}\mathrm{C}$	$T_{\mathrm{m}} = 15.43\,^{\circ}\mathrm{C}$, $\Delta H_{\mathrm{m}} = 15.81\,\mathrm{kJ/mol}$ $T_{\mathrm{C}} = 100.46\,^{\circ}\mathrm{C}$, $\Delta H_{\mathrm{c}} = 0.31\,\mathrm{kJ/mol}$

The X-ray diffraction photographs of well-oriented monodomain samples of the ABC and ABD mixture in the nematic phase, is shown in Fig. 5a, b. The angular distribution of the X-ray diffraction intensities for mixtures ABC and ABD were used to determine the order parameters $\langle P_2 \rangle$ and $\langle P_4 \rangle$ defined by [24, 25]:

$$\langle P_2 \rangle = \left\langle \frac{1}{2}(3\cos^2\theta - 1) \right\rangle, \tag{4}$$

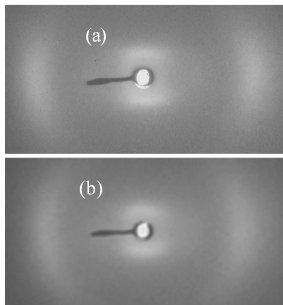$$\langle P_4 \rangle = \left\langle \frac{1}{8}(35\cos^4\theta - 30\cos^2\theta + 3) \right\rangle. \tag{5}$$

Fig. 5. X-ray diffraction photograph from an aligned sample of mixture (a) ABC at $68\,^{\circ}\mathrm{C}$ and (b) ABD at $T = 88\,^{\circ}\mathrm{C}$.

It is to be noted that to determine the order parameters from X-ray diffraction photographs, a χ-scan (i.e. X-ray intensity $I(\chi)$ vs. azimuthal angle χ curve) of the outer diffraction arc for $\chi = 0$ to $\chi = 360^{\circ}$ was first obtained. The measured intensity distribution $I(\chi)$ was then utilized to determine the orientational distribution function $f(\beta)$ and the order parameters $\langle P_2 \rangle$ and $\langle P_4 \rangle$. The peak intensity position which corresponds to $\chi = 0$ was determined from the χ-scan. From the values of $I(\chi)$, the distribution function $f(\beta)$, and the order parameters ($\langle P_2 \rangle$ and $\langle P_4 \rangle$) was calculated following Leadbetter's expression [25]. For the determination of the experimental $f(\beta)$ values and hence the order parameters,

the azimuthal distribution of the X-ray intensities $I(\chi)$ in one quadrant (from $\chi = 0$ to $\chi = 90^{\circ}$) is sufficient. However, in case of X-ray patterns on photographic film, the experimental intensity values over the four quadrants are generally measured and the average values of $I(\chi)$ is used to calculate $f(\beta)$.
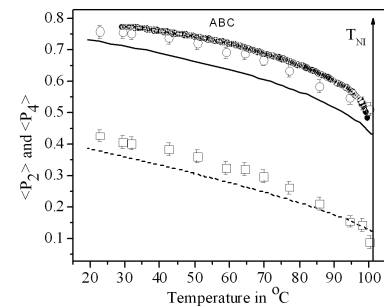

Fig. 6. Temperature variation of $\langle P_2 \rangle$ values for mixture ABC determined from ○ X-ray diffraction measurements, ● birefringence measurement, □ $\langle P_4 \rangle$ from X-ray diffraction measurements, — $\langle P_2 \rangle$ from the Maier–Saupe theory, --- $\langle P_4 \rangle$ from the Maier–Saupe theory. T_{NI} = nematic-isotropic transition temperature. Vertical bar indicates estimated error.

Figures 6 and 7 show the variation of the experimentally determined OOP's with temperature for the two mixtures ABC and ABD, respectively. The experimental $\langle P_2 \rangle$ values are relatively high in the nematic phase compared to the theoretical Maier–Saupe theory, showing the phase to be much more orientationally ordered. Similar higher values of $\langle P_2 \rangle$ are also observed in the OOP values obtained from the birefringence method, which are also included in the respective figures. The agreement between the two sets of order parameters is surprisingly good.

The values of the apparent molecular length and the intermolecular distance D at different temperatures are also measured for the two mixtures studied. The temperature variation of the intermolecular distance, D, for
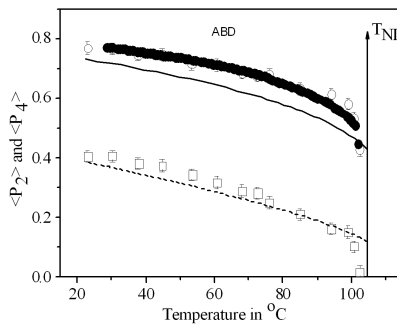
Fig. 7. Temperature variation of $\langle P_2 \rangle$ values for mixture ABD determined from ∘ X-ray diffraction measurements, • birefringence measurement, □ $\langle P_4 \rangle$ from X-ray diffraction measurements, — $\langle P_2 \rangle$ from the Maier–Saupe theory, - - - $\langle P_4 \rangle$ from the Maier–Saupe theory. T_{NI} = nematic-isotropic transition temperature. Vertical bar indicates estimated error.
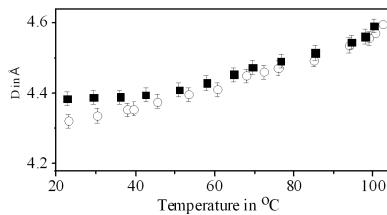

Fig. 8. Temperature dependences of D values for mixtures ABC and ABD. Key to symbols: ■ mix ABC; ∘ mix ABD; vertical bar indicates estimated error.

mixtures ABC and ABD throughout the mesomorphic range are shown in Fig. 8. The variation of D with temperature in the nematic phase is quite appreciable, caused by the increasing thermal vibrations of the chain parts of these molecules. As expected, for both the mixtures, the apparent molecular lengths (l) increase with increasing temperature, and the effect is pronounced near the N–I phase transition (Fig. 9). This increase before the phase transition is once again due to the increasing thermal variations of the chain parts just before the transition.
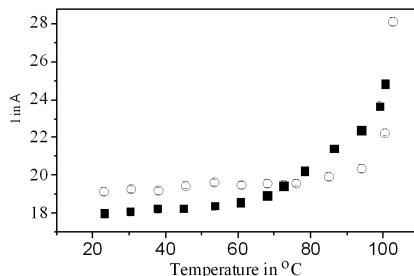

Fig. 9. Temperature dependences of l values for mixtures ABC and ABD. Key to symbols: ■ mix ABC; ∘ mix ABD; vertical bar indicates estimated error.

4. Summary and conclusions

Two tri-component mixtures ABC and ABD for VA mode application were prepared. Both ABC and ABD mixtures are room temperature nematics with a fairly wide operating temperature range. ABC mixture has a slightly improved nematic range over ABD mixture. The optical birefringence, Δn, of these mixtures are in the range of 0.18 to 0.2 at around 30 °C.

The OOP values determined from both the optical birefringence and X-ray diffraction measurements are found to be relatively higher in comparison to the theoretical Maier–Saupe values, indicating high degree of orientational ordering within the phase. X-ray photographs in the nematic phase of both the mixtures reveal the presence of cybotactic groups. The laterally fluorinated constituents A and B of these mixtures, with strong transverse dipole moments may favour the formation of local clusters within the nematic phase thereby forming the cybotactic nematic phase. The temperature variation of the structural parameters — the apparent molecular length, l, and the intermolecular distance, D, shows considerable temperature dependence especially near the nematic–isotropic transition temperature, caused probably due to the increased thermal vibrations of the chain parts of the molecules.

References

[1] C.Y. Xiang, X.W. Sun, X.J. Yin, *J. Appl. Phys.* **37**, 994 (2004).
[2] D.S. Seo, *Liq. Cryst.* **27**, 1147 (2000).
[3] S. Gauza, M. Jiao, S.-T. Wu, P. Kula, R. Dabrowski, X. Liang, *Liq. Cryst.* **35**, 1401 (2008).
[4] M. Schadt, W. Helfrich, *Appl. Phys. Lett.* **18**, 127 (1971).
[5] P. Alvelda, M. Bolotski, I.L. Brown, *Proc. SPIE* **3955**, 109 (2000).
[6] H.C. Huang, B.L. Zhang, H.S. Kwok, P.W. Cheng, Y.C. Chen, *Soc. Info. Disp. Symp. Digest* **36**, 880 (2005).
[7] B.L. Zhang, H.S. Kwok, H.C. Huang, *J. Appl. Phys.* **98**, 123103 (2005).
[8] T.J. Scheffer, J. Nehring, *Appl. Phys. Lett.* **45**, 1021 (1984).
[9] M. Oh-e, M. Ohta, S. Aratani, K. Kondo, in: *15th International Display Research Conference, Asia Display*, 1995, p. 577.
[10] M. Oh-e, K. Kondo, *Appl. Phys. Lett.* **69**, 623 (1996).
[11] V. Reiffenrath, J. Krause, H.J. Plach, G. Weber, *Liq. Cryst.* **5**, 159 (1989).

[12] P. Kirsch, M. Bremer, *Angew. Chem.* **112**, 4384 (2000).

[13] P. Kirsch, M. Bremer, *Angew. Chem., Int. Ed.* **39**, 4216 (2000).

[14] D. Pauluth, K. Tarumi, *J. Mater. Chem.* **14**, 1219 (2004).

[15] B. Bahadur, *Liquid Crystals: Applications and Uses*, Vol. I, World Sci., Singapore 1991.

[16] P.G. de Gennes, J. Prost, *The Physics of Liquid Crystals*, Clarendon Press, Oxford 1993.

[17] S. Charandrasekhar, *Liquid Crystals*, Cambridge University Press, Cambridge 1977.

[18] W. Maier, A. Saupe, *Z. Naturforsch.* **15a**, 287 (1960).

[19] E.C.H. Hsu, J.F. Johnson, *Mol. Cryst. Liq. Cryst.* **20**, 177 (1973).

[20] I. Schröder, *Z. Phys. Chem.* **11**, 449 (1893).

[21] G. Sarkar, M.K. Das, R. Paul, B. Das, W. Weissflog, *Phase Transit.* **82**, 433 (2009).

[22] I. Haller, *Prog. Solid State Chem.* **10**, 103 (1975).

[23] H.P. Klug, L.E. Alexander, *X-ray Diffraction Procedure for Polycrystalline and Amorphous Materials*, Wiley, New York 1974, p. 114, 473.

[24] B. Bhattacharjee, S. Paul, R. Paul, *Mol. Phys.* **44**, 1391 (1981).

[25] A.J. Leadbetter, P.G. Wrighton, *J. Phys. (Paris)* **40**, C3-234 (1979).